Journal of Cell Science 109, 1297-1310 (1996)
Printed in Great Britain © The Company of Biologists Limited 1996
JCS3404

Mutations which block the binding of calmodulin to Spc110p cause multiple mitotic defects

Douglas A. Stirling, Timothy F. Rayner, Alan R. Prescott and Michael J. R. Stark*

Department of Biochemistry, The University, Dundee DD1 4HN, UK

*Author for correspondence

SUMMARY

We have generated three temperature-sensitive alleles of *SPC110*, which encodes the 110 kDa component of the yeast spindle pole body (SPB). Each of these alleles carries point mutations within the calmodulin (CaM) binding site of Spc110p which affect CaM binding in vitro; two of the mutant proteins fail to bind CaM detectably (*spc110-111*, *spc110-118*) while binding to the third (*spc110-124*) is temperature-sensitive. All three alleles are suppressed to a greater or lesser extent by elevated dosage of the CaM gene (*CMD1*), suggesting that disruption of CaM binding is the primary defect in each instance. To determine the consequences on Spc110p function of loss of effective CaM binding, we have therefore examined in detail the progression of synchronous cultures through the cell division cycle at the restrictive temperature. In each case, cells replicate their DNA but then lose viability. In *spc110-124*, most cells duplicate and partially separate the SPBs but fail to generate a functional mitotic spindle, a phenotype which we term 'abnormal metaphase'. Conversely, *spc110-111* cells initially produce nuclear microtubules which appear well-organised but on entry into mitosis accumulate cells with 'broken spindles', where one SPB has become completely detached from the nuclear DNA. In both cases, the bulk of the cells suffer a lethal failure to segregate the DNA.

Key words: *Saccharomyces cerevisiae*, Calmodulin, *SPC110*, *NUF1*, Mitosis, Spindle pole body, Microtubule

INTRODUCTION

Proper nucleation and organisation of microtubules is an essential step in the generation of a mitotic spindle which is competent to segregate sister chromatids during mitosis. Such organisation is achieved by the function of microtubule organising centres (MTOCs). In the yeast *Saccharomyces cerevisiae*, MTOC function is provided by the spindle pole body (SPB), a multi-layered organelle which lies within the nuclear membrane and organises both cytoplasmic and nuclear microtubules (Byers and Goetsch, 1973). During the cell division cycle after Start, the SPB duplicates and as the two SPBs separate, a mitotic spindle is organised between them. While there remains much to be learned about the yeast SPB, considerable progress has been made recently in identifying some of the SPB components and in characterising genes involved in SPB duplication and function (reviewed by Kilmartin, 1994; Snyder, 1994; Winey and Byers, 1993).

The product of *SPC110* (Spc110p), which is allelic with *NUF1* (Mirzayan et al., 1992), is an essential 110 kDa protein with a large central coiled-coil domain and forms a spacer element between the central and inner plaques of the SPB (Kilmartin et al., 1993; Rout and Kilmartin, 1990). The structural role of Spc110p in the SPB is clearly demonstrated by the reduction in the spacing between the central and inner plaques of the SPB which occurs in a predictable manner when its central coiled-coil region is truncated to varying extents (Kilmartin, 1994). In addition to its role as a spacer within the SPB, Spc110p is also a critical target of calmodulin (CaM), a small, essential Ca^{2+}-binding protein which is ubiquitous in eukaryotes (Geiser et al., 1993; Stirling et al., 1994). Thus dominant mutations of *SPC110* can suppress the defects resulting from mutations in the calmodulin gene *CMD1*, Cmd1p and Spc110p interact in the two-hybrid system and the two proteins show direct binding in vitro (Geiser et al., 1993; Stirling et al., 1994). Furthermore, when cells are treated so as to preserve the antigenicity of SPB components, CaM is found to co-localise with other known SPB components, consistent with the presence of a CaM-binding protein at the SPB (Geiser et al., 1993; Stirling et al., 1994). CaM frequently binds to amino acid sequences which can be folded into a basic amphipathic alpha helix (O'Neil and DeGrado, 1990; Török and Whitaker, 1994). Spc110p is predicted to contain such a motif in its carboxyl terminal domain and mutations which map to this region (residues 901-913) block or reduce CaM binding in vitro (Stirling et al., 1994). Binding of CaM to Spc110p is normally an absolute requirement for Spc110p function, since strains relying on single copies of *spc110* alleles encoding products unable to bind CaM detectably in vitro are inviable (Stirling et al., 1994). However, since forms of Spc110p which have been truncated before the CaM binding site can support viability, CaM binding is dispensable in proteins which lack the C-terminal region (Geiser et al., 1993; our unpublished observations). This suggests that CaM binding might be

needed to displace an inhibitory factor or to neutralise the effect of an autoinhibitory domain in Spc110p which also resides in the C-terminal region. In yeast, the role of CaM in Spc110p function is not, however, the only requirement for CaM and genetic studies have indicated that there are at least four separate essential functions (Ohya and Botstein, 1994). One of these additional functions almost certainly involves the nonconventional myosin Myo2p (Brockerhoff et al., 1994).

In this work, we present the characterisation of three different *spc110* conditional alleles. Two of the alleles encode forms of Spc110p which completely fail to bind CaM detectably in vitro and fail to localise CaM to the SPB in vivo at the normal level, while the third mutant protein shows temperature-sensitive in vitro CaM binding. By making use of synchronous cell cultures, we show that these mutants develop highly abnormal patterns of nuclear microtubule organisation at the nonpermissive temperature, indicating that failure to produce a proper mitotic spindle is responsible for the loss of viability seen on shifting cells to the nonpermissive conditions.

MATERIALS AND METHODS

Strains, media and general methods

The strains used in this work are listed in Table 1 and with the exception of TRY124 their generation has been described previously (Stirling et al., 1994). pDS124, encoding a GST fusion to the C-terminus of Spc110p (residues 861-944) but with the C911R mutation, was isolated by screening for the inability to bind ProtA-CaM as previously described (Stirling et al., 1994). An integration plasmid (pTR124) encoding the full length gene incorporating this mutation was constructed and used to generate a strain which relies on a single copy of this gene as the sole source of Spc110p also as described earlier (Stirling et al., 1994). Basic yeast methods and growth media were as described by Kaiser et al. (1994) and yeast transformation was carried out according to the method of Gietz et al. (1992).

Cell cycle synchronisation and FACS analysis

Cell cycle synchronisation was performed by addition of synthetic α-factor to exponentially growing cultures of *MAT***a** strains at a final concentration of 3.5 μg ml^{-1} and arrest in G_1 monitored microscopically by the enrichment in the proportion of unbudded cells. To release the α-factor arrest, cells were harvested, washed once, then resuspended in fresh, prewarmed growth medium containing 0.1 vol. of filter-sterilised medium preconditioned by the growth of an *SST1* strain. To determine survival levels in synchronised cultures, samples were taken at regular intervals, diluted in growth medium, briefly sonicated to aid separation of clumped cells and then an appropriate volume plated on YPD agar. Survival was calculated as the number of colony forming units per ml divided by the cell density in cells per ml (determined by haemocytometer counting) and plotted as the percentage of the initial survival at the time of the temperature shift (% initial survival). The DNA content of cells was determined by flow cytometry of propidium iodide labelled yeast cells using a Becton Dickinson FACSCAN as previously described (Butler et al., 1991).

Immunofluorescence microscopy

Cells were prepared for immunofluorescence microscopy in a number of ways depending on which antigens were being examined. Formaldehyde fixation for visualisation of microtubules alone was as described by Kaiser et al. (1994). For analysis of SPB antigens (Spc90p, Spc110p and CaM), the method of Rout and Kilmartin (1990) was used as previously described (Stirling et al., 1994) except that cells were maintained at their growth temperature at all stages until methanol treatment. Monoclonal antibodies to the Spc90p and Spc110p (anti-110) were kindly provided by John Kilmartin in the form of hybridoma conditioned medium and were used at dilutions of 1 in 2. Affinity purified rabbit polyclonal antibodies against Spc110p (anti-110AP) and yeast CaM antibodies (Stirling et al., 1994) were used at dilutions of 1 in 20 and 1 in 30, respectively. Experiments in which wild-type cells were double-labelled separately with anti-Spc90p/anti-110AP (e.g. Fig. 4) and with anti-110/anti-110AP (not shown) confirmed that both anti-Spc110p antibodies recognised all SPBs defined by anti-Spc90p staining. For visualisation of these primary antibodies, FITC (Sigma) and Texas red (Amersham and Vector Laboratories) conjugated secondary antibodies were employed as indicated in the text. To visualise DNA, the mounting medium contained 1 mg ml^{-1} 4′6-diamidino-2-phenylindole dihydrochloride (DAPI). An Olympus BH-2 fluorescence microscope and T-max 3200 film (Kodak) were used for routine microscopy and photography. Laser scanning confocal microscopy was carried out using a Nikon Microphot-SA microscope equipped with a Bio-Rad MRC600 scan head. When examining the SPB localisation of CaM at 37°C in the *spc110-124* mutant it was not possible to obtain reproducible results. At the restrictive temperature, the mutant cells become highly resistant to cell wall digestion, making this step abnormally variable. This variability, together with the sensitivity to ionic conditions of CaM binding by the *spc110-124* product shown in vitro (see below) are the most likely reason for these difficulties.

For simultaneous visualisation of SPBs, DNA and microtubules, cells were first harvested by rapid centrifugation and fixed briefly by resuspending in 0.1 M potassium phosphate buffer (pH 6.5) containing 3.7% formaldehyde, shaking gently for 15 minutes. The cells were harvested, washed in 0.1 M potassium phosphate buffer and then treated as described above for SPB antigens. These conditions permit visualisation of microtubules whilst sufficiently preserving the antigenicity of the 90 kDa SPB component (Spc90p). The prepared cells were examined using a Zeiss Axioplan fluorescence microscope with a ×100 magnification Plan-Neofluar 1.3 NA objective lens linked to a Photonic Sciences Coolview CCD camera. The software used was Ionvision (Improvision Ltd, Coventry, UK) for image capture and camera control and Adobe Photoshop (Adobe Systems Incorp., Mountain View, CA, USA) for fluorescence channel merging and processing (see Lange et al., 1995).

Western blotting

Preparation of yeast cell protein extracts, SDS-PAGE and western blotting using ProtA-CaM as a probe were carried out as described previously (Stirling et al., 1994) except that incubation of filters with ProtA-CaM and subsequent washing steps were carried out at strictly controlled temperatures as indicated, and all buffers contained 20 mM $MgCl_2$ and 0.1 mM $CaCl_2$. Detection was carried out using ECL (enhanced chemi-luminescence) reagents (Amersham) with Konica X-ray film and quantitated using a Molecular Dynamics densitometer.

RESULTS

spc110 alleles whose products are defective in calmodulin binding

We previously identified a number of mutations in the C-terminal region of Spc110p which affect its ability to bind calmodulin (CaM) in vitro (Stirling et al., 1994) as monitored using ProtA-CaM, a Protein A-calmodulin fusion polypeptide (Stirling et al., 1992). These mutations lie within or very close to a region capable of adopting the basic amphipathic alpha-helical conformation (residues 901-913) typical of CaM

Table 1. Strains

Name	Genotype*	Source
DSY110/1	*MAT***a** *ade2-1 his3 trp1-1::(pDS110)$_1$ leu2 ura3 spc110::LEU2*	Stirling et al. (1994)
DSY111/6	*MAT***a** *ade2-1 his3 trp1-1::(pDS111)$_4$ leu2 ura3 spc110::LEU2*	Stirling et al. (1994)
DSY118/10	*MAT***a** *ade2-1 his3 trp1-1::(pDS118)$_3$ leu2 ura3 spc110::LEU2*	Stirling et al. (1994)
TRY124	*MAT***a** *ade2-1 his3 trp1-1::(pDS124)$_1$ leu2 ura3 spc110::LEU2*	This study

*Subscript numbers indicate the number of copies of the plasmid integrated at *trp1*.

binding sites within target proteins (O'Neil and DeGrado, 1990). Two mutant alleles encoding proteins which were unable to bind CaM in vitro were also unable to support growth of yeast strains when present in single copy as the sole source of Spc110p (*spc110-111* and *spc110-118*). However, strains carrying three (*spc110-118*) or four (*spc110-111*) copies of these genes were viable but temperature-sensitive (Stirling et al., 1994). Each of these alleles contains two point mutations (Table 2), one of which is a valine → acidic replacement which is expected to disrupt the hydrophobic face of the basic amphipathic alpha-helix predicted at the CaM binding site (Stirling et al., 1994). While the *spc110-118* strain grew only slightly slower than wild-type at 26°C, *spc110-111* showed a much reduced growth rate even at this permissive temperature, suggesting a more severe defect (Table 2).

Both these mutations were identified by screening *E. coli* colonies, carrying a library of plasmids expressing the C-terminal region of Spc110p fused to GST, for failure to bind ProtA-CaM. A third isolate (carrying pDS124) also clearly failed to bind ProtA-CaM following lysis of *E. coli* cells on a filter, but on closer analysis by SDS-PAGE and western blotting, expressed a GST-Spc110p fusion protein which seemed to bind ProtA-CaM at a similar level to the equivalent wild-type fusion polypeptide. DNA sequence analysis of pDS124 revealed that it encoded a single amino acid change (C911R) within the proposed Spc110p CaM binding site which might be expected to disrupt CaM binding. We therefore analysed this mutation further by engineering it into a full-length *SPC110* gene and introducing the mutant gene (*spc110-124)* into yeast cells at the *trp1* locus as the sole source of Spc110p, exactly as described previously (Stirling et al., 1994). When present in single copy, the *spc110-124* allele was capable of supporting growth but conferred temperature-sensitivity at 37°C. Thus unlike the *spc110-111* and *spc110-118* alleles, *spc110-124* carries just a single point mutation in the proposed CaM binding site and confers temperature-sensitive (Ts^-) growth in single copy. Like *spc110-118*, growth of the *spc110-124* strain (TRY124) at the permissive temperature of 26°C was only slightly slower than that of a comparable *SPC110* wild-type strain (Table 2).

To determine whether the temperature-sensitivity of *spc110-124* was specifically related to an effect of the mutation on CaM binding, wild-type and *spc110-124* mutant GST-Spc110p fusion proteins were probed on western blots with ProtA-CaM at differing temperatures. Fig. 1 shows that at 26°C, ProtA-CaM binding by the mutant fusion protein (encoded by pDS124) was reduced twofold compared to the wild-type protein. However, although both proteins interacted with ProtA-CaM rather less well at 37.5°C than 26°C, at this higher temperature the signal from the mutant protein was approximately 30-fold weaker than from wild-type. The temperature-sensitivity of in vitro binding at 37.5°C depended on the inclusion of $MgCl_2$ throughout the assay to mimic intracellular conditions, otherwise the reduction in binding by the mutant protein was less marked and evident only at slightly higher temperatures (not shown). Thus the mutant protein interacts with CaM less effectively in vitro and, significantly, the temperature-sensitivity of CaM binding in vitro strongly suggests that the Ts^- phenotype of the *spc110-124* strain is specifically due to reduced CaM affinity under the nonpermissive conditions.

If the defects in the *spc110* strains result directly from reduced affinity for CaM, then CaM overproduction would be predicted to rescue their conditional lethality by improving CaM binding at the ensuing higher intracellular CaM concentration. In fact all three mutant alleles were suppressed by

Table 2. Properties of the conditional *spc110* alleles

Allele	Mutation(s)	Doubling time (minutes) at 26°C*	CaM binding in vitro	Suppression by YEp*CMD1*					
				30°C	33°C	34.5°C	35.5°C	37°C	
spc110-111	V904D, I917S	130.1±5.3	No†	+++	+++	++	+	-	YEp*CMD1*
				+++	+	+	-	-	YEp24
spc110-118	V908E, R913W	109.1±0.5	No†	+++	+++	+++	+++	++	YEp*CMD1*
				+++	+++	++	-	-	YEp24
spc110-124	C911R	109.2±3.3	Yes, Ts^-	+++	+++	+++	+++	+++	YEp*CMD1*
				+++	+++	+++	-	-	YEp24
SPC110	-	99.8±1.6	Yes	+++	+++	+++	+++	+++	YEp24

*Mean ± standard error of two determinations.
†Stirling et al. (1994).

expression of *CMD1* from the *GAL* promoter (Stirling et al., 1994, and data not shown), although suppression of *spc110-111* was incomplete. All three strains were also suppressed by introduction of a high-copy vector carrying *CMD1* (Table 2), although again suppression was essentially complete only for *spc110-118* and *spc110-124*. The fact that elevated dosage or overexpression of *CMD1* is sufficient to rescue the Ts$^-$ phenotype to a significant extent in all three strains strengthens the notion that loss of an effective interaction with CaM largely or wholly accounts for their defects.

Localisation of calmodulin at the SPB in the *spc110* mutants

Given the in vitro data, the *spc110* mutations would be predicted to reduce the level of CaM detectable at the SPBs, particularly at higher growth temperatures. We therefore examined the localisation of calmodulin to the SPBs of wild-type and mutant cells using confocal immunofluorescence microscopy as described previously (Stirling et al., 1994). Unfortunately, we encountered difficulties obtaining reproducible results for the localisation of CaM to the SPBs of mutant cells grown under the non-permissive conditions. However, Fig. 2 shows that at 26°C, CaM is clearly present at the SPBs of wild-type (A) and TRY124 (D) cells. Although CaM was not completely absent from the SPBs in DSY111/6 (*spc110-111*) and DSY118/10 (*spc110-118*) at 26°C (Fig. 2B,C), it was barely detectable. These results are in agreement with the inability to detect significant ProtA-CaM binding to these two mutant proteins in vitro by western blotting at room temperature (see Table 2) and supports the notion that each protein retains some slight, residual level of CaM interaction in vivo. This is consistent with the ability of high-copy *CMD1* or CaM overproduction to suppress the mutations.

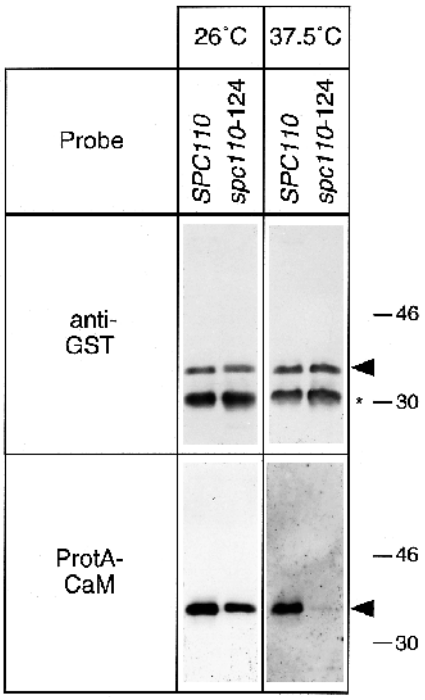

Fig. 1. The C911R mutation in Spc110p confers Ts$^-$ binding of ProtA-CaM in vitro. GST fusion proteins encoding the CaM-binding region from either wild-type *SPC110* or *spc110-124* were expressed in *E. coli*. Following SDS-PAGE and transfer to PVDF membrane, the fusion proteins were probed with either anti-GST antibodies (to confirm equivalent loadings) or ProtA-CaM (to monitor CaM binding efficiency) at either 26°C or 37.5°C. Binding of ProtA-CaM to the mutant polypeptide was vastly reduced relative to the wild-type protein at the higher temperature. The bands denoted by the arrowhead are the full-length GST-Spc110 fusion polypeptides and the anti-GST band denoted by an * is a proteolytic fragment which lacks the Spc110p CaM binding region. The positions of molecular mass standards are indicated on the right in kDa.

Asynchronous cultures of *spc110^{ts-}* cells arrest with aberrantly organised microtubules

To examine the effect of the *spc110* mutations, exponentially growing cultures of the three *spc110* strains were transferred to 37°C. Under these conditions, each strain ceased proliferation within roughly 2 hours, suggesting an arrest within the first cell division cycle following the temperature shift. This conclusion was confirmed by synchronous culture experiments (see below). After 240 minutes under the restrictive conditions, samples were examined microscopically. While wild-type control cells appeared normal (Fig. 3A), the three mutant cultures consisted mainly of much larger cells, each with a bud of similar size to the mother cell (i.e. a 'dumb-bell' morphology). Immunofluorescence microscopy revealed that the arrangement of nuclei and microtubules in these cells was abnormal (Fig. 3B-D). In DSY118/10 (Fig. 3C) and TRY124 (Fig. 3D), the nuclei were predominantly near or through the bud neck and were associated with highly irregular, branched arrays of microtubules. In addition, the amount of microtubules present appeared greater than in wild-type cells. This phenotype was also observed in DSY111/6 (Fig. 3B), but in addition a sub-population of cells was seen in which the arrangement of microtubules was even more complex and sometimes apparently broken in two (Fig. 3B, two cells at top right). In some of these cells, the nucleus failed to migrate to the bud neck (not shown in Fig. 3). These arrest phenotypes are indicative of one or more defects in the execution of mitosis resulting from abnormal organisation of the microtubules.

Spc110p localisation is not disrupted in the *spc110* mutants

Spc110p has been shown to form a spacer element between the central and inner plaques of the SPB (Kilmartin et al., 1993). The mutant arrest phenotypes observed could therefore arise for a number of reasons related to SPB function, including incorrect SPB assembly, duplication or separation, or defective attachment of microtubules to the inner face of the SPB. To address some of these possibilities, confocal immunofluorescence microscopy was used to examine localisation of Spc110p to the SPBs in the three mutant strains. In cells double-labelled with anti-Spc90p and affinity purified polyclonal antibodies against Spc110p, there was no detectable difference between wild-type and *spc110* cells which had been incubated at either 26°C or at 37°C for at least two hours, sufficient time for SPB duplication to occur. Fig. 4 shows that at 37°C, in each case *all* SPBs identified by anti-Spc90p staining showed apparently normal levels of anti-Spc110p reactivity. Since Spc90p is located in both the inner and outer plaques of the SPB and most anti-Spc90p staining occurs on the cytoplasmic face (Rout and Kilmartin, 1990), it is unlikely that the *spc110* mutations could block recognition of SPBs by the

anti-Spc90p antibody. We therefore conclude that the *spc110* mutations do not block assembly of Spc110p into the SPB and that the reduced amount of CaM at the SPBs of DSY111/6 and DSY118/10 does not result from absence of Spc110p at the restrictive temperature. However, we cannot rule out by this method either that the level of mutant Spc110p present at the SPBs is somewhat reduced or that it has been incorrectly inserted into the SPB. Since in many cells two spindle pole bodies were observed in association with the nucleus (not shown), it is also likely that SPB duplication can occur in the mutants at the restrictive temperature, as discussed below.

Synchronous cultures of *spc110* mutants arrest as large dumb-bells

To gain a more detailed understanding of the *spc110* defect, we carried out a series of experiments using the most and least severe mutant strains and a wild-type control (DSY111/6, TRY124 and DSY110/1, respectively). Although we have not studied the *spc110-118* strain DSY118/10 in the same detail, its behaviour seems most similar to TRY124 (not shown). Exponentially growing cultures were synchronised at Start by incubation with the mating pheromone α-factor and then released from the cell cycle block at either the permissive or restrictive temperatures. Progression from the block was monitored by regular sampling for at least four hours, examining cell morphologies, measuring cell survival, using FACS analysis to measure DNA content and quantifying the spatial relationships of SPBs, microtubules and nuclear DNA by immunofluorescence microscopy.

At 37°C, a clear progression from unbudded to small budded to large budded and back to unbudded cells was seen as wild-type cells completed their first cell cycle following release from

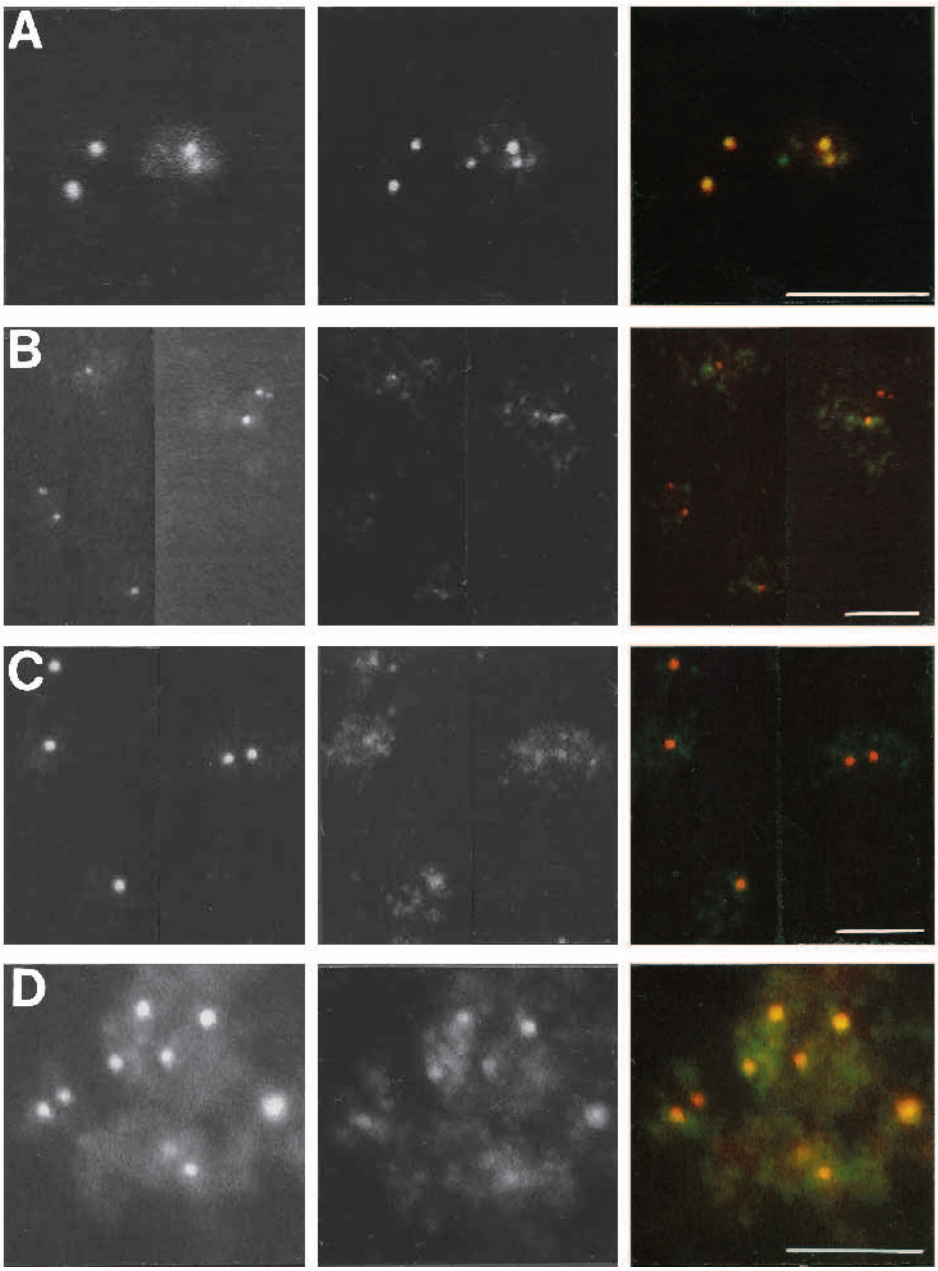

Fig. 2. Localisation of calmodulin at the SPB. DSY110/1 (A), DSY111/6 (B), DSY118/10 (C) and TRY124 (D) cells grown at 26°C were double labelled with anti-Spc90p/anti-CaM (A,B,C) or anti-Spc110p/anti-CaM (D) primary antibodies followed by anti-mouse IgG-TRITC/anti-rabbit IgG-FITC (A,B,D) or anti-mouse IgG-FITC/anti-rabbit IgG-TRITC (C) secondary antibodies, then examined by confocal microscopy. SPB labelling (with anti-Spc90p or anti-Spc110p) is shown on the left, calmodulin labelling in the centre and merged images on the right, where SPB and CaM staining are shown in red and green, respectively. Yellow indicates points of co-localisation of the two antigens. The observed localisation of CaM at the SPBs was unaffected by whether the anti-Spc90p or anti-Spc110p monoclonal antibodies were used as SPB markers (not shown). Bars, 5 μm. Note the different magnifications used in A to D: there was no noticeable difference in the sizes of the spots detected by the antibodies in each strain.

the α-factor block (Fig. 5). However, in both the mutants, this progression was halted with the appearance of the 'dumb-bell' phenotype following the peak of large budded cells, a morphology which persisted for several hours. In addition, a small percentage of other aberrant cells with multiple buds appeared in the mutants after prolonged incubation. At the permissive temperature, all three strains behave essentially identically, completing one cell cycle and embarking on the next within the period examined (data not shown). One exception to this is the appearance, at low frequency, of aberrant multi-budded cells in DSY111/6 at the permissive temperature. Notably, the abundance of this aberrant morphology was maximal around the point of cell division, suggesting a defect in cytokinesis leading to unseparated cells which then embark on a second cell cycle.

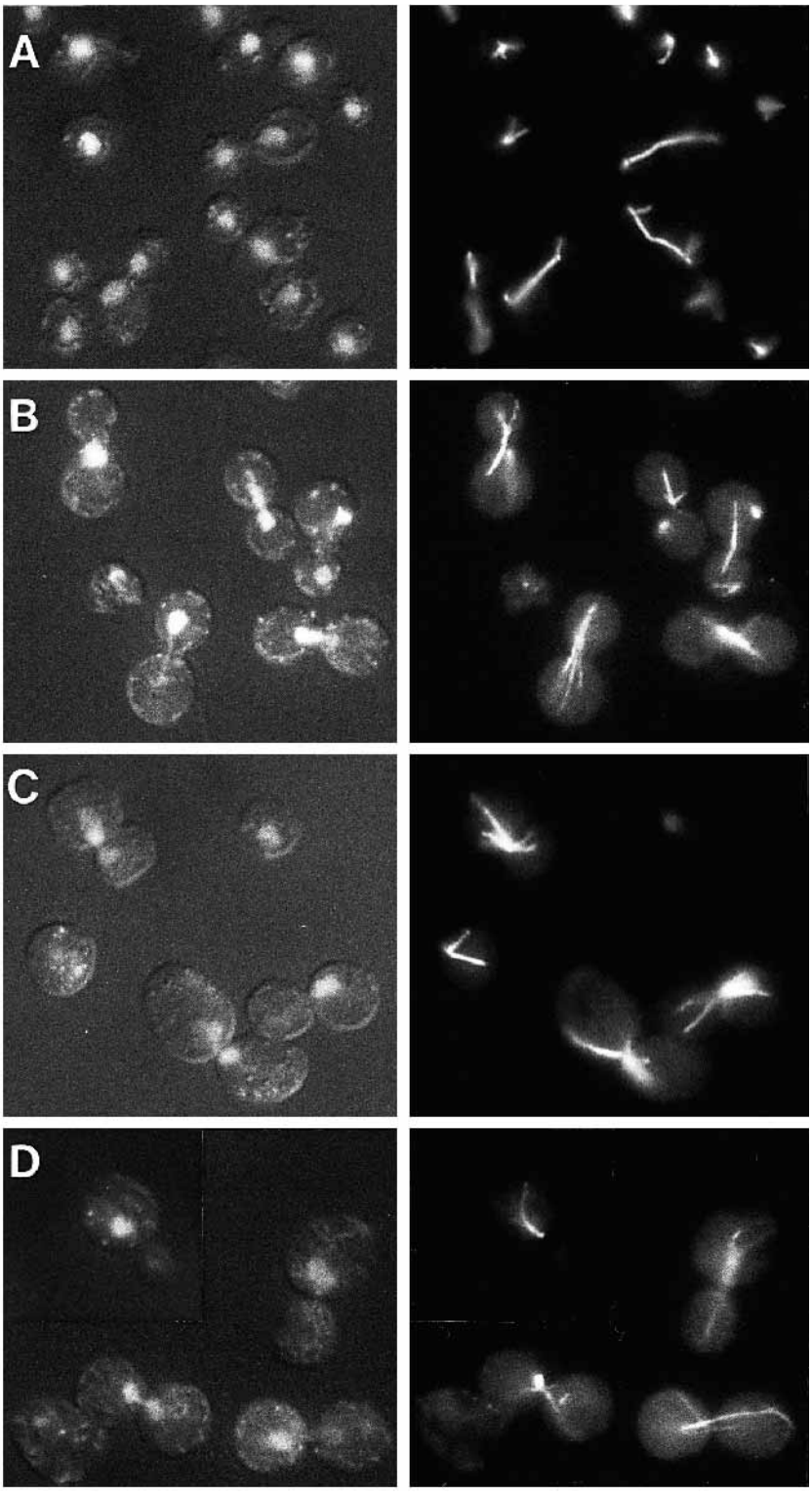

Fig. 3. Asynchronous arrest of spc110 mutants. Samples of exponentially growing cultures of strains DSY110/1 (A), DSY111/6 (B), DSY118/10 (C) and TRY124 (D) were shifted to 37°C for 240 minutes and prepared for microscopy. Cells were viewed at ×1,000 magnification by both differential interference contrast with additional UV illumination to visualise DAPI-stained DNA and cell morphology simultaneously (left-hand panels), and tubulin was visualised by FITC immunofluorescence microscopy (right-hand panels).

spc110 mutants lose viability after completion of DNA replication

Following release from α-factor, FACS analysis showed that the DNA content in wild-type cells at 37°C shifted from 1C to 2C as DNA replication progressed, with a subsequent shift back towards 1C as the cells divided (Fig. 6A). The completion of S-phase approximately corresponded to the peak in abundance of small budded cells (compare Figs 5 and 6A). This was also observed in the mutants grown at the permissive temperature, showing that DNA replication was not delayed (not shown). However, although DNA replication occurred on cue in the mutants at 37°C, the shift back to 1C DNA content was considerably less marked. This confirms that the defect in these strains takes effect at a point after the commitment to and completion of S-phase. At later time points in both mutants, the 2C FACS peak broadened markedly, a feature generally associated with an increase in cell size, and in DSY111/6 a small population of cells with much less than 1C DNA content appeared (Fig. 6B). This latter feature became even more marked upon even longer incubation at the non-permissive temperature (not shown) and suggests the generation of aploid cells.

Asynchronous cultures of both DSY111/6 and TRY124 cells lose viability on prolonged incubation at the non-permissive temperature (not shown). In synchronous cultures, the initial viability of both strains was maintained through S-phase but then rapidly decreased after the onset of the abnormal 'dumbbell' morphology (Fig. 5). For DSY111/6 cells, this decrease began immediately following S-phase as indicated by FACS analysis, but in TRY124 there was a delay of around 50 minutes before cells began to lose viability. This could simply reflect that *spc110-111* has a more severe defect than *spc110-124* such that the point at which cells become inviable is

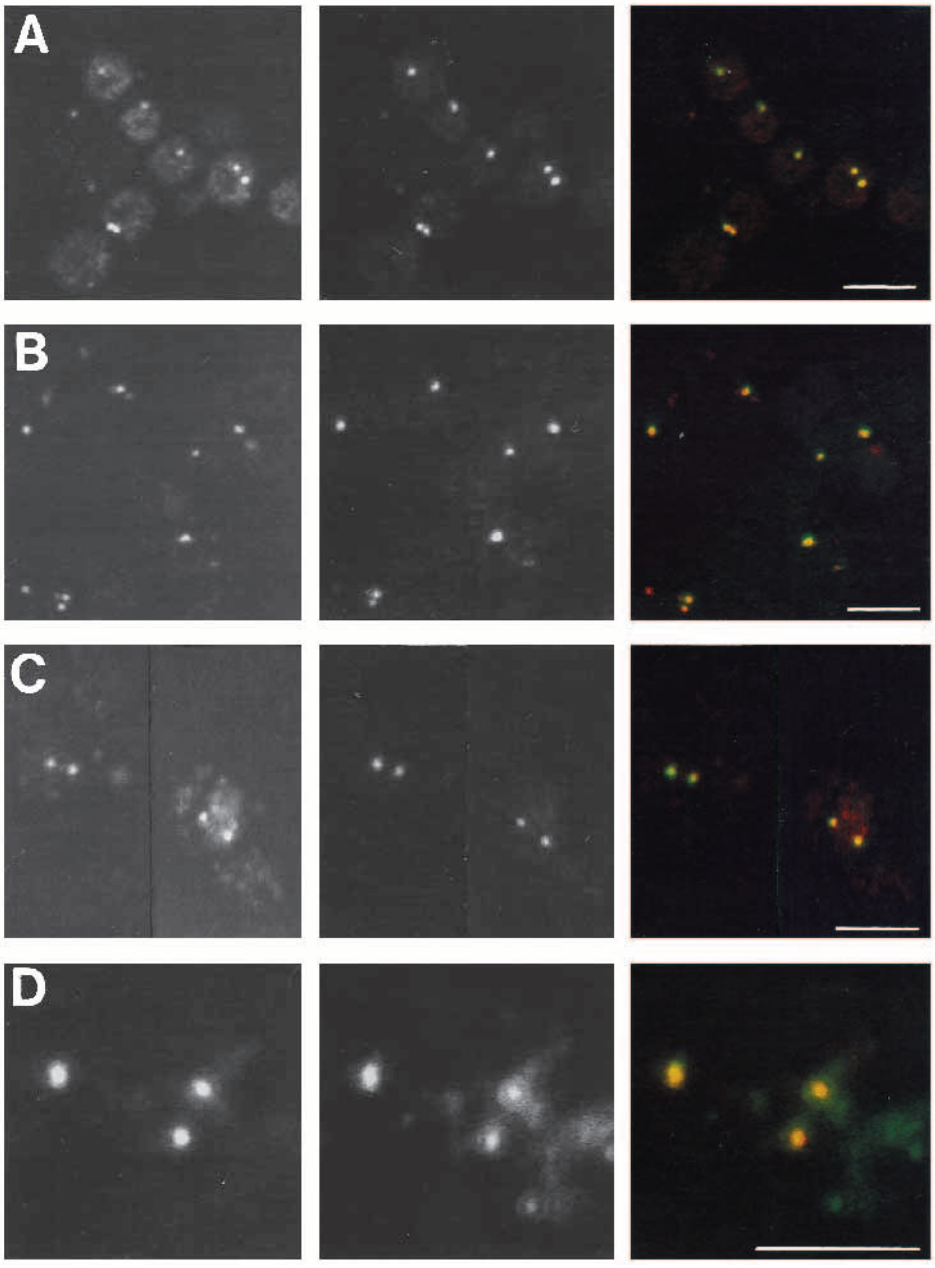

Fig. 4. Spc110p remains localised at the SPB in spc110 mutants. DSY110/1 (A), DSY111/6 (B), DSY118/10 (C) and TRY124 (D) cells grown at 37°C were double-labelled with monoclonal anti-Spc90p/affinity-purified polyclonal anti-Spc110 primary antibodies followed by anti-mouse IgG-FITC/anti-rabbit IgG-TRITC secondary antibodies, then examined by confocal microscopy. Anti-Spc110p labelling is shown on the left, anti-Spc90p labelling in the centre and merged images on the right, where the anti-Spc110p and anti-Spc90p signals are shown in red and green, respectively. Yellow indicates points of co-localisation of the two antigens. Bars, 5 μm. Note the different magnifications used in A to D: there was no noticeable difference in the sizes of the spots detected by the antibodies in each strain.

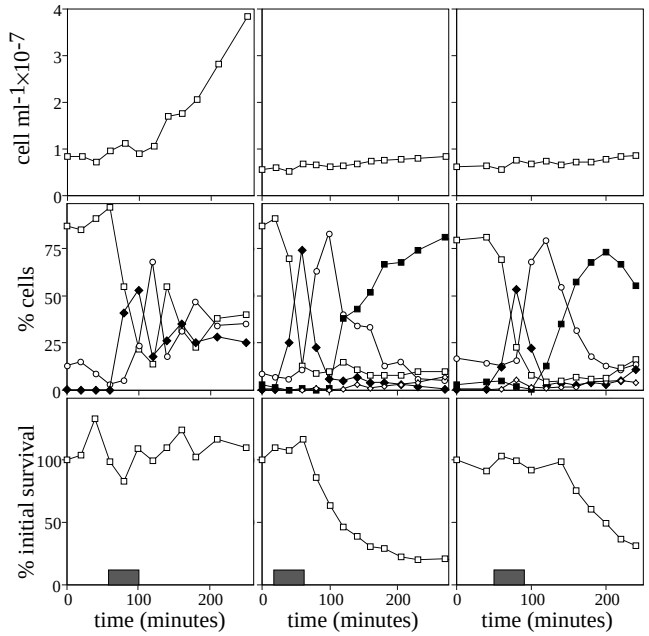

Fig. 5. *spc110* strains arrest and lose viability after DNA replication. Cultures of DSY110/1, DSY111/6 and TRY124 were synchronised using α-factor and released at 37°C at time zero. Cell density (upper panel), cell morphology (central panel), and percentage survival (lower panel) of (left to right) DSY110/1, DSY111/6 and TRY124 were monitored for at least four hours following release from the α-factor block. In the central panel, the different morphologies are represented by the following symbols: □, unbudded cells; ◆, cells with a small bud; ○, cells with a large bud; ■, dumb-bells; ◇, other aberrant morphologies (see text). The shaded bar on the *x*-axis indicates the duration of S-phase in each experiment as determined by flow cytometric analysis of the same cultures (see Fig. 6). For each of the strains the time taken for the cell population to bud after α-factor release varied slightly between experiments, but the timing of S-phase relative to the initiation of budding was always essentially identical in each case.

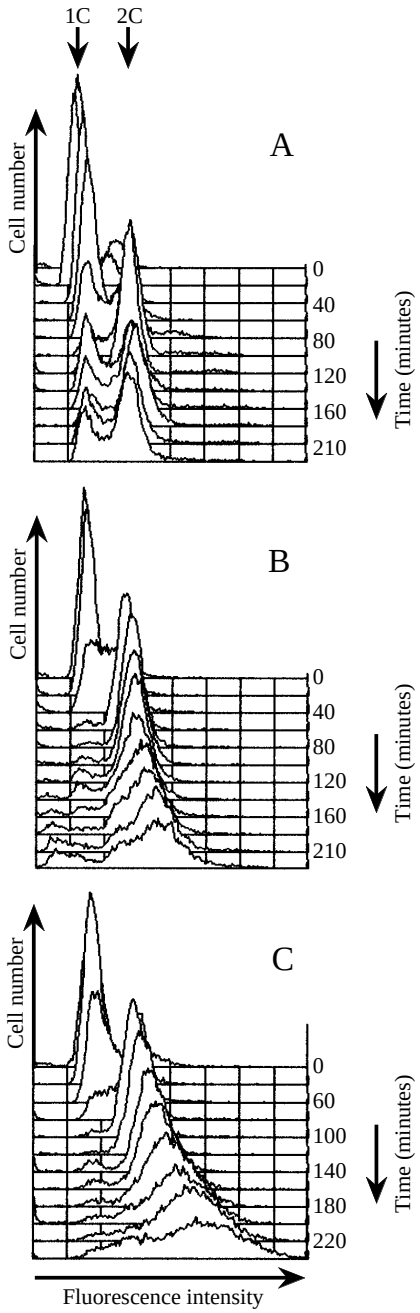

Fig. 6. *spc110* mutant cells arrest with replicated DNA. Samples taken from the synchronous cultures shown in Fig. 5 were examined by FACS analysis at regular intervals following release from α-factor block at 37°C to measure their DNA content. (A) DSY110/1; (B) DSY111/6; (C) TRY124. For each strain, graphs of relative cell number (*y*-axis) versus relative DNA content (*x*-axis) from twelve time points are overlaid with the latest time point at the front. The positions of the 1C and 2C peaks are indicated and the times of sampling shown at the right.

reached more rapidly, possibly being a consequence of the significant difference in the restrictive temperatures of the two strains (Table 2). Alternatively, the more severe mutant might be defective for an additional, temporally distinct event which is not affected in *spc110-124* cells. Either way, failure to complete the later stages of the cell cycle in both these strains is accompanied by loss of viability.

spc110-124 cells arrest with abnormal microtubule organisation

The arrangement of SPBs, microtubules and nuclear DNA were classified and quantified in synchronous cultures for approximately four hours after release from α-factor arrest by immunofluorescence microscopy. Fig. 7 presents the results in the form of area graphs, showing the variations in the proportion of cells in each morphological class over the timecourse. Examples of each major class of normal and abnormal morphologies are also presented as CCD micrographs in Figs 8 to 10, showing merged SPB, tubulin and DNA images for each cell.

In control *SPC110* wild-type cultures, there was a progression in the morphologies of cells released from α-factor in the following order as expected: (i) unbudded with one SPB (Fig. 8A,B); (ii) budded with one SPB (Fig. 8C,D); (iii) budded with two separated SPBs linked by a short spindle (Fig. 8E-H;‘normal metaphase’); (iv) budded, with a longer spindle linking the two SPBs and nuclear DNA stretched through the neck (Fig. 8I;‘anaphase’); (v) two SPBs separated to opposite

ends of the budded cell, connected by a long spindle and with nuclear DNA equally divided into mother and bud (Fig. 8J;'telophase'). This was a cyclical progression repeating after about 140 minutes.

On release from α-factor, the first indication of a defect in TRY124 was the appearance of more extensive arrays of cytoplasmic microtubules compared with wild-type (e.g. compare Fig. 8A,B with Fig. 9A,B). After budding and DNA replication, the cells appeared to proceed at least partly into mitosis; two SPBs were usually visible and the nucleus frequently migrated to the bud neck. In wild-type cells, mitotic spindles consisted mainly of well-defined bundles of nuclear microtubules stretched between two SPBs at opposite sides of the nucleus (e.g. Fig. 8E-J). However, in *spc110-124* cells this arrangement was severely disrupted and cytoplasmic microtubules predominated, often branching out in extensive arrays from the nucleus into both mother and daughter cells (Fig. 9). The nuclear microtubules were improperly organised, sometimes branched and often with little or no evidence of a mitotic spindle (Fig. 9F-I,N). The SPBs were frequently only partially separated (Fig. 9F-I); indeed, some of the large-budded cells apparently containing a single SPB (Fig. 9C,D) may represent duplicated SPBs which cannot be resolved by light microscopy. The majority of *spc110-124* cells showed many of these phenotypes, which we have termed 'abnormal metaphase' and which can be summarised as partially separated SPBs, inappropriate organisation of cytoplasmic and nuclear microtubules, and the replicated nuclear DNA either adjacent to or inserted into the neck region.

A small proportion of cells progressed past the abnormal metaphase, reaching anaphase or telophase but usually with abnormal distributions of microtubules and often having divided their DNA unequally between the mother and daughter cells (Fig. 9K). Other cells showed a phenotype which we have termed a 'broken spindle', in which one SPB was disassociated from the main body of the DNA and pulled into the bud (Fig. 9L,M). This SPB usually remained associated with microtubules and sometimes with small fragments of DAPI-stained DNA (not shown). Finally, a small but significant population of *spc110-124* cells lacking a nucleus but containing both microtubule arrays and a single SPB appeared late in the experiment (Fig. 9P), possibly the product of cells executing an abnormal anaphase in which the replicated DNA failed to divide. This corresponds to the increase in the fraction of unbudded cells around 200-240 minutes after release from α-factor (Fig. 7C).

The *spc110-111* mutation leads predominantly to 'broken spindles'

In contrast to TRY124, strain DSY111/6 (*spc110-111*) displayed a more complex collection of morphologies. In particular, three predominant characteristics differed from *spc110-124*. Firstly, the earliest abnormal morphology was the appearance of *unbudded* cells with separated SPBs, often connected by a short spindle which appeared quite normal (Fig. 10A). A minority of cells also showed this morphology at the permissive temperature (not shown). Secondly, the normal progression from unbudded cells with a single SPB to budded cells

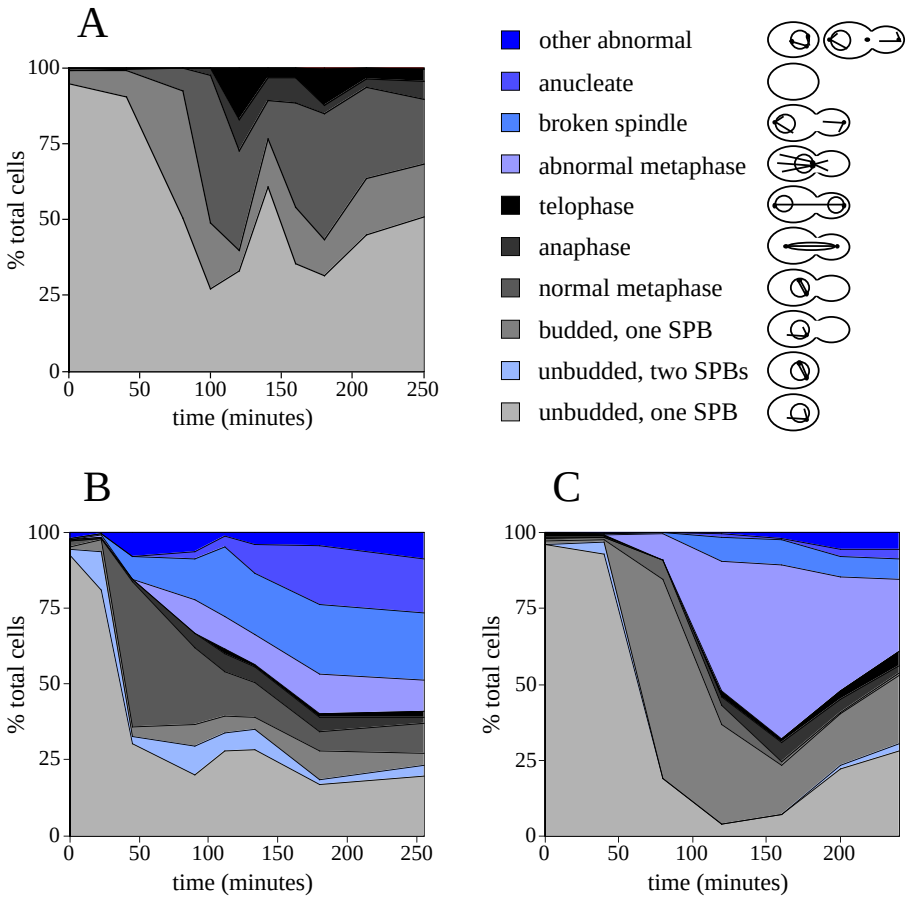

Fig. 7. Appearance of abnormal cell morphologies in *spc110-111* and *spc110-124* mutant synchronous cultures. Cultures of (A) DSY110/1, (B) DSY111/6 and (C) TRY124 were synchronised using α-factor and released at 37°C. Samples from each were taken over a 4 hour timecourse and cells categorised as indicated based on their overall morphology and patterns of tubulin, SPB and DNA staining observed by fluorescence microscopy. The proportion of cells at each time point corresponding to each of the categories indicated are plotted as area graphs. At each point, a minimum of 200 cells were examined. The 'other abnormal' class in both *spc110* mutants includes a diverse group of morphologies, none of which alone constituted more than 2% of the total. The proportion of unbudded cells with a single SPB never fell below 27%. However, since *all* cells underwent DNA replication after release from α-factor (Fig. 6) this reflects the lack of perfect synchrony rather than indicating that some cells failed to release from the block. Figs 8-10 show CCD micrographs which illustrate examples of each category and are discussed in the text.

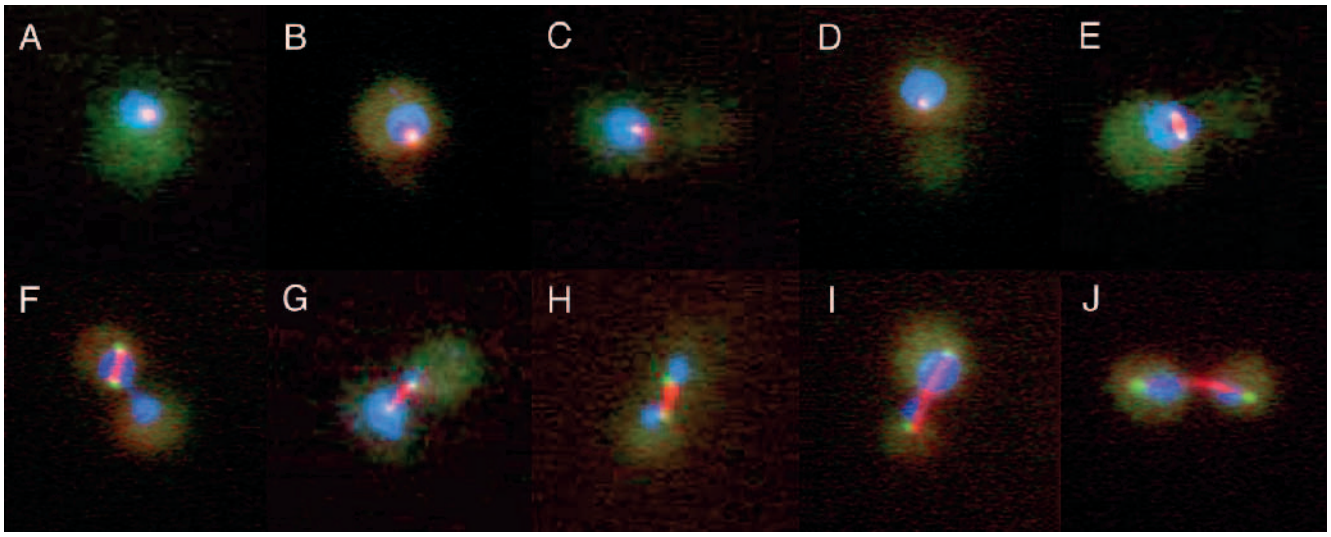

Fig. 8. Cells of DSY110/1 at various stages of the cell division cycle. Examples of DSY110/1 cells (*SPC110* wild type) selected from the experiment of Fig. 7A are shown to indicate the normal progression through mitotic cell division as follows: (A,B) unbudded with one SPB; (C,D) budded with one SPB; (E,F,G,H) normal metaphase; I, anaphase; J, telophase. The nucleus is shown in blue to represent DAPI fluorescence, the anti-tubulin signal in shown in red and the SPB signal in green. Note that SPB fluorescence appears either yellow or white where tubulin or tubulin plus DNA, respectively, co-localise with the SPB, while purple indicates co-localisation of tubulin and DNA.

with a single anti-Spc90p-staining focus was not seen; almost all budded cells had more than one such focus. In many cases, it was noted that in these cells the spindle appeared polarised (Fig. 10B). One interpretation of these data is that the coordination of SPB duplication, spindle formation and bud emergence is altered in this mutant.

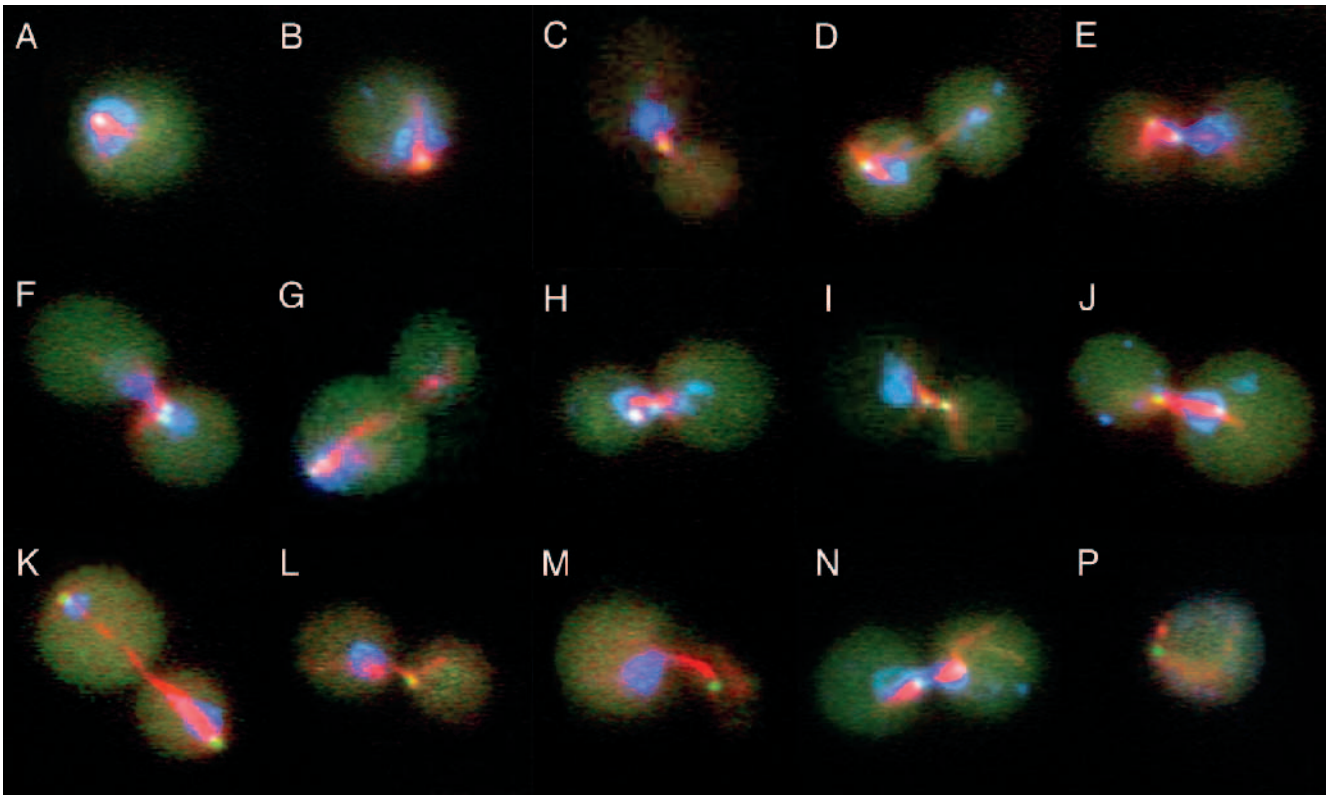

Fig. 9. Cells of TRY124 at various stages of the cell division cycle. Examples of TRY124 cells (*spc110-124* wild type) selected from the experiment of Fig. 7C are shown to indicate the development of abnormal cellular phenotypes following release from α-factor arrest. (A,B))Unbudded with one SPB; (C,D) large budded cells with one SPB visible; (E,F,G,H,I) abnormal metaphase; (J) anaphase with a 'polarised' spindle; (K) telophase with a polarised spindle; (L,M) broken spindle; N, abnormal metaphase; P, unbudded, anucleate with one SPB. See Fig. 8 for details of colour representation.

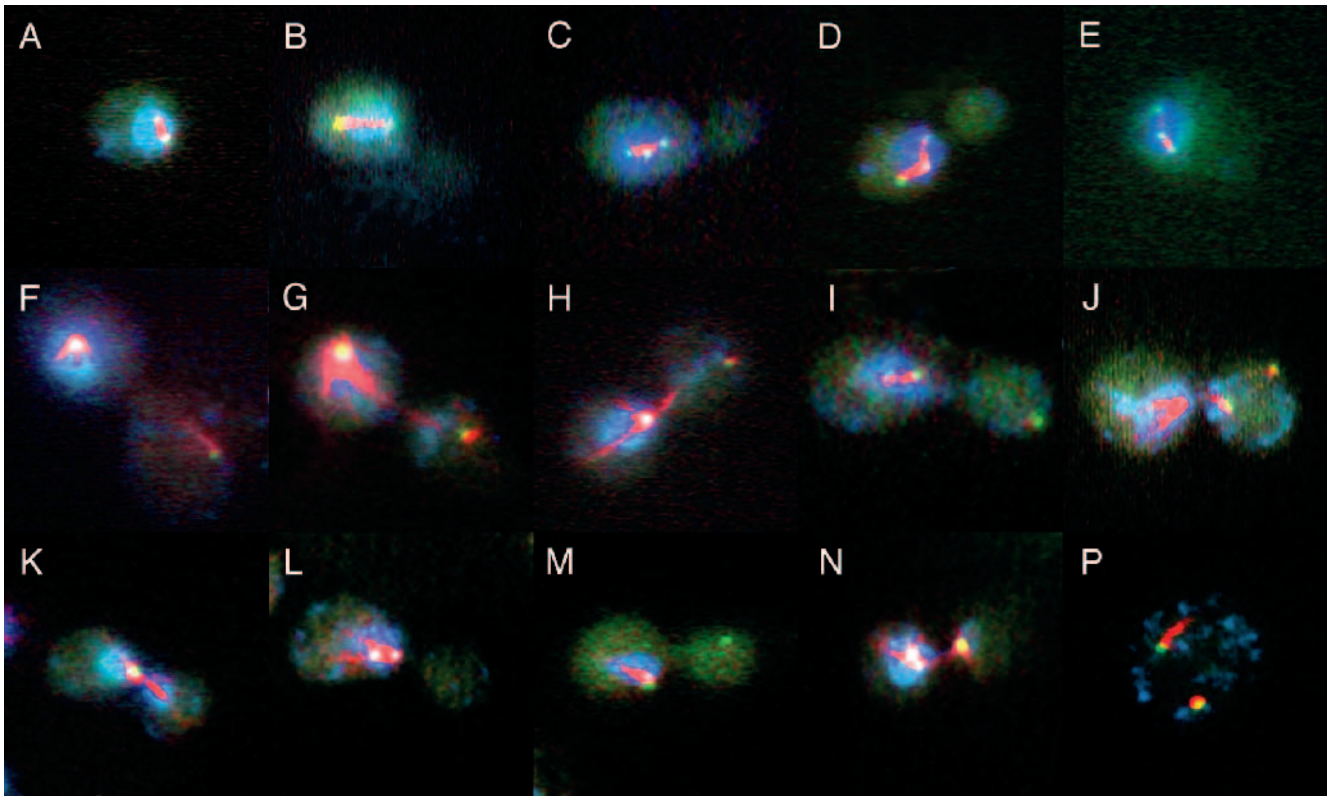

Fig. 10. Cells of DSY111/6 at various stages of the cell division cycle. Examples of DSY111/6 cells (*spc110-111* wild-type) selected from the experiment of Fig. 7B are shown to indicate the development of abnormal cellular phenotypes following release from α-factor arrest. (A) Unbudded with two SPBs; (B) budded with two SPBs with 'polarised' spindle; (C,D,E) budded with apparently three SPBs; (F,G,H) large budded cells with a broken spindle; (I,J) large budded cells with three SPBs and a broken spindle; (K,L) abnormal metaphase; (M,N) abnormal metaphase with three SPBs; P, unbudded, anucleate cell with two SPBs. See Fig. 8 for details of colour representation.

Thirdly, cells with a range of budding morphologies apparently containing more than two SPBs were present. Although we describe these cells as having three SPBs on the basis of reactivity with the anti-Spc90p-specific antibody, we cannot of course rule out the possibility that the additional anti-Spc90p staining spots are fragments of SPBs or aggregates of SPB components which have not been assembled properly. In Fig. 7B some of these cells fell into the abnormal metaphase and broken spindle classes with the remainder included in the 'other aberrant' class. However, taken as a whole, cells with more than two SPBs were first significant (8.6%) 45 minutes after release from α-factor at the non-permissive temperature in unbudded and small budded cells, where the three SPBs were usually associated with the nucleus. Bundles of nuclear microtubules which appeared quite normal often linked all the SPBs (Fig. 10C-E) although sometimes one was only weakly attached to the microtubules (Fig. 10E). At later times when a maximum of 14.3% of cells had more than two SPBs (255 minutes) their arrangement was even more variable, with one or more of them usually dissociated from the DNA and not linked to the others by microtubules (Fig. 10I,J,M,N). In some cells, there were two SPBs in the presumed mother cell (containing the nucleus) with another SPB in the bud (Fig. 10I,M,N), whilst in other cells there were two SPBs in the bud (Fig. 10J). None of these morphologies was present in DSY111/6 cells grown at the permissive temperature (not shown).

In addition to these specific features, the predominant abnormal arrest phenotype of DSY111/6 cells was the presence of broken spindles, resulting in a lack of segregation of replicated chromosomes between mother and daughter cells (Fig. 7). This was a minor phenotype in TRY124, but represented the major aberrant phenotype at 2 hours and around half of all aberrant phenotypes seen in the *spc110-111* strain by 4 hours after α-factor release (Fig. 7). In contrast to TRY124, the definition of broken spindles was complicated by the additional SPBs often present in DSY111/6 cells; we therefore classified a cell as having a broken spindle if one SPB was detached from the microtubule array and the remaining SPB(s) and microtubules were not clearly displaying the abnormal metaphase morphology discussed above. Broken spindles appeared in cells with the nucleus distal (Fig. 10F,G) or proximal (Fig. 10H-J) to the bud neck. A small proportion of cells with the abnormal metaphase morphology were also present (Fig. 10K-N).

Another major class of cells appearing in synchronous cultures of DSY111/6 at 37°C were those with little or no nuclear DNA (Fig. 10P). These cells, together with a large proportion of the other unbudded cells, were almost certainly generated by the Zymolyase treatment necessary for immunofluorescence analysis from large dumb-bells in which the spindle had broken and where, in many cases, one or more SPBs had dissociated from the DNA and migrated into the bud.

For example, after 180 minutes at the restrictive temperature only 8% of DSY111/6 cells appeared unbudded when sonicated cells were examined, whereas immunofluorescence microscopy indicated a total of 37.6% unbudded cells (16.9% unbudded with one SPB, 1.4% unbudded with two SPBs and 19.3% unbudded anucleate: Fig. 7B). The value of 20.6% for cells with broken spindles at this time point must therefore be a substantial underestimate. This discrepancy between the level of unbudded cells in the same samples treated in the two different ways was also evident in the analysis of synchronous cultures of DSY111/6 at the permissive temperature where, for example, Zymolyase treatment was found to convert a population with 21% unbudded cells to one in which this value was 73% in the most extreme instance (not shown). This phenomenon was not seen with TRY124 or the wild-type control and is again suggestive of a cytokinesis defect at the permissive temperature. Taken together, the simplest interpretation of the data for DSY111/6 at the *restrictive* temperature suggests progression from an apparently 'normal metaphase' configuration, via a broken spindle to a population of aploid and 2C unbudded cells as cells with the broken spindle morphology become separable by Zymolyase. The abnormal metaphase configuration does not appear to be part of this progression, but observation of the SPB and tubulin organisation in real time would probably be required to demonstrate this unambiguously.

DISCUSSION

The use of conditional *spc110* mutants defective in the ability of Spc110p to bind CaM has indicated that CaM binding is required for the successful execution of mitosis in *S. cerevisiae*. Under the nonpermissive conditions, both mutants examined here in detail successfully replicated their DNA and remained viable at least until S-phase was complete. However, they showed abnormal patterns of microtubule formation and SPB behaviour, leading ultimately to either the abnormal metaphase or the broken spindle phenotypes discussed above and consequent failure, in most cells, to segregate the DNA. The relative predominance of these two configurations varied between the mutants: while *spc110-111* showed predominantly the broken spindle phenotype, *spc110-124* and *spc110-118* presented the abnormal metaphase as the major aberrant morphology. These phenotypes do not therefore appear to correlate with the apparent severity of each *spc110* mutation on CaM binding in vitro. Thus both *spc110-111* and *spc110-118* seem to cause a major loss of CaM binding efficiency in vitro compared with *spc110-124*, but *spc110-118* and *spc110-124* shared the same predominant terminal phenotype (abnormal metaphase). However, the terminal phenotype *does* correlate with the ability of each mutation to be suppressed by additional copies of *CMD1* or CaM overproduction, in that *spc110-118* and *spc110-124* were essentially fully suppressed whereas *spc110-111* was not, suggesting either that it may have a more severe CaM binding defect in vivo or that its mutations affect a second aspect of Spc110p function.

If Spc110p mediates the mitotic requirement for CaM, it might be thought that the phenotypes of our *spc110* mutants and of *cmd1* mutants which are specifically defective in CaM's mitotic function should be similar. In fact both of the major terminal phenotypes which we see are superficially reminiscent of those seen in *cmd1-101* mutant strains at the nonpermissive temperature. The *cmd1-101* mutant is dependent for viability on overproduction of the C-terminal half of yeast calmodulin and at higher temperatures showed three predominant arrest phenotypes (Sun et al., 1992). Two of these (types I and III) are consistent with the abnormal metaphase category which we have described, while the third (type II) resembles our broken spindle phenotype, with the SPB often pulled away from the bulk of the nuclear DNA. Similar phenotypes have also been reported for the *cmd1C* intragenic complementation group of Ts^- CaM mutants (Ohya and Botstein, 1994). However, an important difference is that in the *cmd1-101* strain SPB duplication did not occur in the majority of cells (i.e. types I and III) and most microtubule configurations were therefore monopolar (Sun et al., 1992). The Ts^- *cmd1-1* allele also led to loss of viability during mitosis, accumulated a significant proportion of aploid cells and showed examples of branched, uneven and 'broken' spindles similar to some of those observed in this study. However, the majority of spindles elongated without obviously breaking and were well organised relative to those seen in the *spc110* mutants; the abnormal metaphase phenotype was evidently not observed (Davis, 1992). Conversely, yeast dependent on a mutant synthetic calmodulin gene (SynCaM) also showed examples of SPBs apparently dissociated from the nucleus (Harris et al., 1994), one of the features of the broken spindle phenotype described here. One feature of *spc110-111* was that cell separation was apparently defective at both the permissive and restrictive temperatures, such that Zymolyase treatment converted a high proportion of large-budded cells into unbudded cells. Since the timing of cytokinesis is dependent on entry of the nucleus into the bud (Yeh et al., 1995), nuclear entry may be delayed in *spc110-111* even at the permissive temperature as well as when the broken spindle phenotype at the restrictive temperature blocks nuclear transit completely. The *cmd1-1* mutant also showed a cytokinesis defect (Davis, 1992). Thus while the *spc110* and *cmd1* mutants show some features in common, the variety of defects seen in each case make it difficult to compare the phenotypes precisely.

The terminal phenotypes of our *spc110* mutants also share some properties with other mutants known to affect the SPB, principally in their failure to segregate the DNA in the majority of cells. However, the terminal phenotype of both *spc110* mutants examined in this study seem distinct from that of any other known mutant affecting the SPB (see Snyder, 1994, for a review). Thus mutations such as *cdc31* and *mps1* block SPB duplication and lead to formation of monopolar spindles, but although a proportion of the *spc110* mutant cells appear to have only a single SPB, the majority have two distinct SPBs. *ndc1* and *mps2* mutations also interfere with SPB duplication, producing in each case a defective daughter SPB. In the case of *ndc1*, the defective daughter SPB was observed to segregate away from the mass of DNA into the bud (Yeh et al., 1995) in a manner reminiscent of the broken spindle phenotype. However, *mps1* and *mps2* strains accumulate cells with polyploid DNA contents after 4-6 hours at the restrictive temperature, but the *spc110* strains described here do not. Like *spc110-111*, *esp1* mutant strains lose viability on entry into mitosis and show a structural failure of the mitotic spindle (McGrew et al., 1992). Furthermore, mutations which affect other components associated with the SPB and mitotic spindle

such as Nuf2p (Osborne et al., 1994) and the microtubule motor proteins Kar3p, Cin8p and Kip1p (Hoyt et al., 1992; Roof et al., 1992) do not show the gross distortions of microtubule organisation which we see in the *spc110* mutants. Loss of function of the motor proteins also causes failure of SPB separation, resulting in side by side SPBs in the nuclear envelope (Hoyt et al., 1992; Roof et al., 1992). However, in the *spc110* mutants SPB separation can occur, but in the abnormal metaphase phenotype is generally far from complete.

Why might CaM binding by Spc110p be required for the formation of a normal yeast mitotic spindle? Simple models are that CaM binding is required either for proper duplication of the SPB or for assembly of Spc110p into the new SPB. However, our data do not provide evidence to support such models. Firstly, during S-phase when SPB duplication should already have occurred, the majority of cells have at least two foci of anti-Spc90p staining, consistent with the presence of two SPBs. Secondly, without exception we found that under the restrictive conditions Spc110p was localised to every SPB defined in this way. This suggests that both SPB duplication and assembly of Spc110p into the new SPB occurs in the mutant cells. Yeast SPB duplication is a conservative step in which the newly-formed SPB is usually directed into the bud (Vallen et al., 1992). When a spindle was present in the mutant cells it frequently showed a non-uniform distribution of nuclear microtubules (e.g. Fig. 9K). This might suggest that while Spc110p can be assembled into the new SPB at the nonpermissive temperature, the new SPB is nonetheless defective in some way. Similarly, in cells showing the broken spindle phenotype the bulk of the microtubules appear to remain associated with the unseparated nucleus (e.g. Fig. 10F-J). Given the mutant phenotypes which we observe and the known location of Spc110p in the SPB (Kilmartin et al., 1993), more likely models for the function of CaM binding to Spc110p include a role in the anchoring of the SPB in the nuclear envelope or in the attachment of nuclear microtubules to the inner face of the SPB. Support for such contentions is provided by the dissociation of SPBs from the mass of DNA and/or the bulk of the microtubules in *spc110-111* and the failure to form a proper spindle at all in *spc110-124*. However, further work would be required to prove either of these two possibilities definitively and in particular, where the SPB has become detached from the DNA we cannot resolve from our data whether it has also become detached from the nuclear envelope.

A major consequence of the *spc110* mutations is the presence of greater numbers of microtubules than normal. Hyperaccumulation of microtubule bundles has also been noted in a yeast strain dependent on a mutant synthetic calmodulin (SynCaM; Harris et al., 1994). One explanation for this could be if the SPB were a major site of microtubule disassembly and this process was defective at the nonpermissive temperature. The MTOC has been proposed as a site of microtubule disassembly in the mitotic spindle of other eukaryotic cells (Mitchison and Salmon, 1992). While it is not yet clear whether this is also true in yeast, a defect in a component of the nuclear face of the SPB could clearly affect such a process. Conversely, an increase in the number of nucleation sites at the SPB or other changes in microtubule dynamics in the mutants could also explain the higher levels of microtubules. Hyperpolymerisation of microtubules has also been noted in quite different situations where the function of the mitotic spindle is perturbed (e.g. loss of kinesin-like protein function; Hoyt et al., 1992) and so could be a more general phenomenon.

The pathways to the broken spindle and abnormal metaphase phenotypes exhibited by the *spc110* mutants show significant differences: thus the *spc110-111* strain was able to generate normal-looking, uniform bundles of nuclear microtubules at earlier times following α-factor release but showed a more rapid onset of lethality, whereas the majority of *spc110-124* cells rarely developed anything reminiscent of a mitotic spindle and yet remained viable for rather longer. It is therefore legitimate to ask whether they are two manifestations of the same defect or whether they represent two quite different effects on Spc110p function. Since both mutants characterised here show both phenotypes to some extent, it could be argued that they are two manifestations of the same defect. On the other hand, since *spc110-111* is not fully suppressed by CaM overproduction or elevated *CMD1* dosage, it may have additional effects on Spc110p function which bias the phenotype towards the broken spindle outcome. Given the two quite different progressions of events, we therefore favour the latter model: on this hypothesis *spc110-111* can produce a mitotic spindle but it is non-functional, whereas *spc110-124* generally fails to produce a mitotic spindle at all. Since cells monitor spindle formation via a checkpoint just prior to mitosis (Hoyt et al., 1991; Li and Murray, 1991), this may explain the longer viability of *spc110-124* cells despite their more abnormal microtubule arrangements. Thus *spc110-111* appears to generate an apparently normal spindle which breaks when pulled, leading to complete dissociation of one SPB from the bulk of the DNA. Conversely, *spc110-124* fails generally to produce a spindle at all and few cells show elongated spindles. This hypothesis could be tested by asking whether deletion of a checkpoint gene such as *MAD1* (Hardwick and Murray, 1995; Li and Murray, 1991) hastened the demise of *spc110-124* cells in synchronous culture. This checkpoint was apparently intact at least at the permissive temperature in all the *spc110* mutants since cells displayed no obvious hypersensitivity to nocodazole (not shown).

One observation peculiar to the *spc110-111* mutant was the relatively large proportion of cells in which the appearance of two clearly-separated foci of Spc90p staining, often organising a short spindle, *preceded* bud emergence. Perhaps even more strikingly, at the restrictive temperature the *spc110-111* strain essentially bypassed the 'unbudded, one SPB' stage corresponding to post-START cells with either unduplicated SPBs or duplicated but unseparated SPBs (see Fig. 7). In the *spc110-124* mutant under the same conditions, roughly 70% of cells had the latter phenotype by 80 minutes following α-factor release (Fig. 7C), showing it to be a stage which most cells passed through. There are at least two possible explanations for this. Either there is a defect in the co-ordination of normal SPB duplication and bud emergence in *spc110-111* cells, or else an additional, distinct SPB is formed abnormally, before the normal SPBs have duplicated or separated sufficiently to be resolved by immunofluorescence microscopy. Such cells could be the fore-runners of cells with three SPBs which were observed later following α-factor release, the appearance of which is consistent with the second model. Indeed, if normal SPB separation was delayed in the *spc110-111* strain, a high proportion of the budded cells with *two* anti-Spc90p foci (classified as'normal metaphase' in Fig. 7B) could potentially also

represent cells with an extra SPB. Either way, in the *spc110-111* mutant there is a clear defect in the behaviour of the SPBs early in the cell cycle and, in the second scenario, this could readily account for some of the defects seen. The presence of an additional, abnormal SPB early in the cell cycle specifically in *spc110-111* cells is also consistent with their distinct, predominant terminal phenotype (broken spindle) when compared with the other two mutants. However, since the cells remain fully viable at this stage (Fig. 6), such a proposed defect is clearly reversible and might only become lethal at later times as cells attempt mitosis. Unbudded cells with two anti-Spc90p foci were also evident at the permissive temperature, but in this case many budded cells with a single anti-Spc90p focus were observed, indicating that the majority of cells passed through the 'budded, one SPB' morphology. This suggests that there was not a defect in SPB duplication in most cells at the permissive temperature (not shown).

Our analysis of these *spc110* mutants emphasises the vital role of CaM in the correct execution of mitosis in *S. cerevisiae*, demonstrating the importance of CaM for establishing and maintaining a functional mitotic spindle through its interaction with Spc110p. Further investigation should establish whether CaM has a structural or regulatory role in these events.

We thank Barbara Spruce, Chris Hutchison and Ian Kill for help with CCD microscopy, Alison Sparks for help with FACS analysis and John Kilmartin for monoclonal antibodies specific for SPB components and for helpful comments. This work was carried out with support from the Wellcome Trust (Project Grant 036234/Z/92/Z). T.F.R. is the recipient of a Research Studentship from the Biotechnology and Biological Sciences Research Council.

REFERENCES

Brockerhoff, S. E., Stevens, R. C. and Davis, T. N. (1994). The unconventional myosin, Myo2p, is a calmodulin target at sites of cell growth in *Saccharomyces cerevisiae*. *J. Cell Biol*. **124**, 315-323.

Butler, A. R., White, J. H. and Stark, M. J. R. (1991). Analysis of the response of *Saccharomyces cerevisiae* cells to *Kluyveromyces lactis* toxin. *J. Gen. Microbiol*. **137**, 1749-1757.

Byers, B. and Goetsch, L. (1973). Duplication of the spindle plaques and integration of the yeast cell cycle. *Cold Spring Harbor Symp. Quant. Biol*. **38**, 123-131.

Davis, T. N. (1992). A temperature-sensitive calmodulin mutant loses viability during mitosis. *J. Cell Biol*. **118**, 607-617.

Geiser, J. R., Sundberg, H. A., Chang, B. H., Muller, E. G. D. and Davis, T. N. (1993). The essential mitotic target of calmodulin is the 110-kilodalton component of the spindle pole body in *Saccharomyces cerevisiae*. *Mol. Cell. Biol*. **13**, 7913-7924.

Gietz, R. D., St Jean, A., Woods, R. A. and Schiestl, R. H. (1992). Improved method for high efficiency transformation of intact yeast cells. *Nucl. Acids Res*. **20**, 1425.

Hardwick, K. G. and Murray, A. W. (1995). Mad1p, a phosphoprotein component of the spindle assembly checkpoint in budding yeast. *J. Cell Biol*. **131**, 709-720.

Harris, E., Watterson, D. M. and Thorner, J. (1994). Functional consequences in yeast of single-residue alterations in a consensus calmodulin. *J. Cell Sci*. **107**, 3235-3249.

Hoyt, M. A., Totis, L. and Roberts, B. T. (1991). *S. cerevisiae* genes required for cell cycle arrest in response to loss of microtubule function. *Cell* **66**, 507-517.

Hoyt, M. A., He, L., Loo, K. K. and Saunders, W. S. (1992). Two *Saccharomyces cerevisiae* kinesin-related gene products required for mitotic spindle assembly. *J. Cell Biol*. **118**, 109-120.

Kaiser, C., Michaelis, S. and Mitchell, A. (1994). *Methods in Yeast Genetics*. *A Cold Spring Harbour Laboratory Course Manual*. Cold Spring Harbor Laboratory Press, New York.

Kilmartin, J. V., Dyos, S. L., Kershaw, D. and Finch, J. T. (1993). A spacer protein in the *Saccharomyces cerevisiae* spindle pole body whose transcript is cell cycle regulated. *J. Cell Biol*. **123**, 1175-1184.

Kilmartin, J. V. (1994). Genetic and biochemical approaches to spindle function and chromosome segregation in eukaryotic microorganisms. *Curr. Opin. Cell Biol*. **6**, 50-54.

Lange, B. M. H., Sherwin, T., Hagan, I. M. and Gull, K. (1995). The basics of immunofluorescence video-microscopy for mammalian and microbial systems. *Trends Cell Biol*. **5**, 328-332.

Li, R. and Murray, A. W. (1991). Feedback control of mitosis in budding yeast. *Cell* **66**, 519-531.

McGrew, J. T., Goetsch, L., Byers, B. and Baum, P. (1992). Requirement for *ESP1* in the nuclear division of *Saccharomyces cerevisiae*. *Mol. Biol. Cell* **3**, 1443-1454.

Mirzayan, C., Copeland, C. S. and Snyder, M. (1992). The *NUF1* gene encodes an essential coiled-coil related protein that is a potential component of the yeast nucleoskeleton. *J. Cell Biol*. **116**, 1319-1332.

Mitchison, T. J. and Salmon, E. D. (1992). Poleward kinetochore fiber movement occurs during both metaphase and anaphase-A in newt lung cell mitosis. *J. Cell Biol*. **119**, 569-582.

O'Neil, K. T. and DeGrado, W. F. (1990). How calmodulin binds its targets: sequence independent recognition of amphiphilic α-helices. *Trends Biochem. Sci*. **15**, 59-64.

Ohya, Y. and Botstein, D. (1994). Diverse essential functions revealed by complementing yeast calmodulin mutants. *Science* **263**, 963-966.

Osborne, M. A., Schlenstedt, G., Jinks, T. and Silver, P. A. (1994). Nuf2, a spindle pole body-associated protein required for nuclear division in yeast. *J. Cell Biol*. **125**, 853-866.

Roof, D. M., Meluh, P. B. and Rose, M. D. (1992). Kinesin-related proteins required for assembly of the mitotic spindle. *J. Cell Biol*. **118**, 95-108.

Rout, M. P. and Kilmartin, J. V. (1990). Components of the yeast spindle and spindle pole body. *J. Cell Biol*. **111**, 1913-1927.

Snyder, M. (1994). The spindle pole body of yeast. *Chromosoma* **103**, 369-380.

Stirling, D. A., Petrie, A., Pulford, D. J., Paterson, D. T. W. and Stark, M. J. R. (1992). Protein A-calmodulin fusions: a novel approach for investigating calmodulin function in yeast. *Mol. Microbiol*. **6**, 703-713.

Stirling, D. A., Welch, K. A. and Stark, M. J. R. (1994). Interaction with calmodulin is required for the function of Spc110p, an essential component of the yeast spindle pole body. *EMBO J*. **13**, 4329-4342.

Sun, G. H., Hirata, A., Ohya, Y. and Anraku, Y. (1992). Mutations in yeast calmodulin cause defects in spindle pole body functions and nuclear integrity. *J. Cell Biol*. **119**, 1625-1639.

Török, K. and Whitaker, M. (1994). Taking a long, hard look at calmodulin's warm embrace. *BioEssays* **16**, 221-224.

Vallen, E. A., Scherson, T. Y., Roberts, T., Vanzee, K. and Rose, M. D. 1992. Asymmetric mitotic segregation of the yeast spindle pole body. *Cell* **69**, 505-515.

Winey, M. and Byers, B. (1993). Assembly and functions of the spindle pole body in budding yeast. *Trends Genet*. **9**, 300-304.

Yeh, E., Skibbens, R. V., Cheng, J. W., Salmon, E. D. and Bloom, K. (1995). Spindle dynamics and cell cycle regulation of dynein in the budding yeast, *Saccharomyces cerevisiae*. *J. Cell Biol*. **130**, 687-700.

(Received 22 December 1995 - Accepted 15 March 1996)